Formation and Structure of Gel Networks from $Si(OEt)_4$/$(MeO)_3Si(CH_2)_3NR'_2$ Mixtures ($NR'_2 = NH_2$ or $NHCH_2CH_2NH_2$)

Nicola Hüsing and Ulrich Schubert*

Institut für Anorganische Chemie, Technische Universität Wien, Getreidemarkt 9, A-1060 Wien, Austria

Rita Mezei and Peter Fratzl

Erich Schmid Institut der Österreichischen Akademie der Wissenschaften & Montanuniversität Leoben, Jahnstr. 12, A-8700 Leoben, Austria

Bernhard Riegel and Wolfgang Kiefer

Institut für Physikalische Chemie, Universität Würzburg, Am Hubland, D-97074 Würzburg, Germany

Dagmar Kohler and Werner Mader

Institut für Anorganische Chemie der Universität Bonn, Römerstr. 164, D-53117 Bonn, Germany

Received October 20, 1998. Revised Manuscript Received November 18, 1998

Monolithic silica aerogels modified by amino-substituted organic groups with bulk densities between 0.07 and 0.16 g cm^{-3} were prepared by sol−gel processing of $Si(OEt)_4$/$(MeO)_3Si(CH_2)_3NR'_2$ mixtures ($NR'_2 = NH_2$ or $NHCH_2CH_2NH_2$), followed by drying of the wet gels with supercritical CO_2. The $Si(OEt)_4$/$(MeO)_3Si(CH_2)_3NR'_2$ ratio was varied between 9:1 and 6:4. The $\equiv Si(CH_2)_3NR'_2$ groups were completely incorporated in the aerogels in each case. Raman spectroscopic investigations showed that the precursors were rapidly consumed upon addition of water to the alkoxysilane mixtures. Gelling was slowed with an increasing portion of $(MeO)_3Si(CH_2)_3NR'_2$. The structure of the aerogels was investigated by nitrogen sorption, small-angle X-ray scattering, and transmission electron microscopy. The polarity of the inner surface of the aerogels was rather low. The particle radii were in the range of 6.0−6.3 nm, the fractal dimension in the range of 1.3−1.6, and the BET surface area in the range of 300−430 m^2 g^{-1}, rather independent of the $Si(OEt)_4$/$(MeO)_3Si(CH_2)_3NR'_2$ ratio. The only exception was an aerogel prepared from 90% $Si(OEt)_4$ and 10% $(MeO)_3Si(CH_2)_3NH_2$, which contains significantly larger primary particles and a smaller specific surface area. The results were interpreted that both precursor silanes are involved in the build-up of the aerogel network, contrary to results with organically substituted alkoxysilanes $R'Si(OR)_3$ without basic properties.

Introduction

Silica aerogels[1] modified by nonfunctional or functional organic groups[2,3] can be prepared by sol−gel processing of $R'Si(OR)_3$/$Si(OMe)_4$ mixtures followed by supercritical drying of the wet gels. The organic groups R′ employed so far had no or only weakly basic properties, such as unsubstituted alkyl or aryl groups, or chloro-, thio-, phosphino-, carbamato-, glycidoxy- or methacryloxyalkyl groups. For the discussions in this paper these groups will be abbreviated as R_{nb} (nb = nonbasic) and the corresponding alkoxysilanes as $R_{nb}Si(OR)_3$. Sol−gel processing of the $R_{nb}Si(OR)_3$/$Si(OMe)_4$ mixtures under base-catalyzed conditions is a two-step process in which the basic gel network is nearly exclusively built from $Si(OMe)_4$ (TMOS). In the network-forming stage, the organically substituted alkoxysilane $R_{nb}Si(OR)_3$ acts as a cosolvent. Only in the second stage of the process are the $R_{nb}SiO_{3/2}$ units condensed on the inner surface of the then existing silica gel network. Inorganic−organic hybrid aerogels prepared from $R_{nb}Si(OR)_3$/$Si(OMe)_4$ mixtures therefore have the same structural features as aerogels prepared from $Si(OR)_4$

(1) Recent review article on the chemistry of aerogels: Hüsing, N.; Schubert, U. *Angew. Chem.* **1998**, *110*, 22; *Angew. Chem., Int. Ed.* **1998**, *37*, 22.

(2) Schwertfeger, F.; Glaubitt, W.; Schubert, U. *J. Non-Cryst. Solids* **1992**, *145*, 85. Schubert, U.; Schwertfeger, F.; Hüsing, N.; Seyfried, E. *Mater. Res. Soc. Symp. Proc.* **1994**, *346*, 151. Schwertfeger, F.; Hüsing, N.; Schubert, U. *J. Sol-Gel Sci. Technol.* **1994**, *2*, 103. Hüsing, N.; Schwertfeger, F.; Schubert, U.; Tappert, W. *J. Non-Cryst. Solids* **1995**, *186*, 37. Hüsing, N.; Schubert, U. *J. Sol-Gel. Sci. Technol.* **1997**, *8*, 807.

(3) Hüsing, N.; Schubert, U.; Misof, K.; Fratzl, P. *Chem. Mater.* **1998**, *10*, 3024.

10.1021/cm980756l CCC: $18.00
Published on Web 01/29/1999

Table 1. Preparation of the Wet Gels

sample	precursors [g, (mmol)] $Si(OEt)_4$	$R_bSi(OR)_3$	MeOH	water	gel time, t_g [min]
AMMO10	12.42 (69)	1.38 (8)	21.95 (685)	5.40 (300)	12
AMMO20	11.91 (57)	2.56 (14)	23.58 (736)	4.68 (270)	15
AMMO30	9.72 (47)	3.59 (20)	24.95 (779)	4.46 (248)	22
AMMO40	7.81 (38)	4.48 (25)	26.16 (816)	4.09 (227)	30
AEAPS10	13.53 (65)	1.60 (7)	22.81 (712)	5.06 (281)	50
AEAPS20	10.60 (51)	2.83 (13)	24.87 (776)	4.37 (243)	30

alone. The *kind* of R_{nb} has no severe influence on the network formation and the network structure, only the fractal dimension of the primary particles is influenced by the polarity of the functional group of the "cosolvent" $R_{nb}Si(OR)_3$.

When the $R_{nb}Si(OR)_3$ *portion* is increased, the gel times become longer, there is increased shrinkage during supercritical drying and incomplete incorporation of the organic groups, the inner surface becomes less polar, and there is a larger compression of the network during N_2 adsorption. The main structural changes are an increasing size of the primary particles and, associated with that, lower specific surface areas. Sol−gel processing of the two-component alkoxysilane mixtures was initiated by adding the whole amount of water and catalyst necessary for the hydrolysis and condensation of both compounds to alcoholic solutions of the silane mixtures. The structural phenomena result from the larger amount of water and catalyst acting on TMOS in the first stage of the reaction, due to the delayed reaction of $R_{nb}Si(OR)_3$.[3]

In this paper we describe the extension of this work to organo(trialkoxy)silanes in which the organic group contains a strongly basic substituent ($R_bSi(OR)_3$; b = basic). The employed trialkoxysilanes $R_bSi(OR)_3$ were $(MeO)_3Si(CH_2)_3NH_2$ (AMMO) and $(MeO)_3Si(CH_2)_3$-$NHCH_2CH_2NH_2$ (AEAPS). We will mainly focus on the development of the microstructure during sol−gel processing compared with the systems derived from R_{nb}-$Si(OR)_3$.

Experimental Section

Sol−Gel Processing of $R_bSi(OR)_3/Si(OR)_4$ Mixtures. The aerogels were prepared as previously described,[2,3] but no catalyst was added. Tetraethoxysilane (TEOS), $R_bSi(OMe)_3$, and methanol were mixed in a flask. An amount of methanol was added corresponding to a theoretical density of the final aerogel of 0.100 g cm^{-3} ($d_{theor} = [(1 - x)m_{SiO_2} + xm_{RSiO_{3/2}}]/(V_{Si(OEt)_4} + V_{RSi(OMe)_3} + V_{H_2O} + V_{ROH})$). To start the sol−gel reactions, the amount of water necessary for the complete hydrolysis of the alkoxy groups was added (Table 1). The sol was stirred for 5 min and then transferred to cylindrical polyethylene vessels 1.5 cm in diameter and 4.5 cm in height.

Supercritical Drying of the Wet Gels. The resulting gels were aged without solvent exchange at 30 °C for 7 d (starting from the time of adding water). Supercritical drying was then performed by using a Polaron 3100 critical point dryer. The alcohol was first replaced by CO_2, then the temperature and pressure were raised above the critical point of CO_2 ($T_c = 31$ °C, $p_c = 7.29$ MPa). The resulting aerogels were monolithic cylinders of white, opaque appearance and had the typical aerogel properties with low densities and high porosities.

The samples are labeled as follows: The letters identify the kind of functional unit incorporated into the silica matrix by using the acronym of the parent silane (AMMO or AEAPS). The following number represents the portion of $R_bSi(OR)_3$ (in mol %) in the starting mixture of the alkoxysilanes. For example, AMMO20 is an aerogel prepared from a mixture of 80 mol % $Si(OEt)_4$ and 20 mol % $(MeO)_3Si(CH_2)_3NH_2$.

Table 2. Structural Characteristics of the Aerogels

sample	nitrogen sorption: BET surf. area, σ [m^2 g^{-1}]	C	small-angle X-ray scattering: particle radius, R [nm]	fractal dimen, D	$3/(R\sigma)$ [g cm^{-3}]
AMMO10	184	42	*a*	*a*	
AMMO20	291	49	6.09 ± 0.22	1.26 ± 0.17	1.69
AMMO30	426	35			
AMMO40	381	40	6.29 ± 0.27	1.55 ± 0.22	1.25
AEAPS10	295	93	6.05 ± 0.14	1.48 ± 0.10	1.68
AEAPS20	288	60	6.12 ± 0.13	1.53 ± 0.10	1.70

[a] R and D cannot be obtained from the scattering curve of this sample; see the text.

Characterization. The physical data of the aerogels are given in Table 2.

The shrinkage during aging and drying was determined by measuring the dimensions of the cylindrical gel body before and after drying. The bulk density was calculated from the mass and the volume of the monolithic samples. The composition of the aerogels was determined by elemental analysis of C, N, Si, and H. Karl Fischer titrations were performed with a Mettler DL18 Karl Fischer titrator. Thermal analyses were carried out with a Shimadzu DSC-50 and TGA-50 analyzer in air.

A Micromeritics Sorptomat ASAP 2400 was used for the nitrogen sorption studies. The samples were preheated overnight at 110 °C before each measurement. The specific surface area was determined by the Brunauer, Emmett, Teller (BET) method at 77.4 K in the partial pressure range of $0.01 < p/p_0 < 0.25$ (five-point BET). The total pore volume was obtained from the N_2 desorption isotherm. For the calculation of the C parameter, only the pressure range of $0.05 < p/p_0 < 0.25$ was used.

The setup for the Raman measurements consisted of a Bruker IFS 120 HR FTIR spectrometer equipped with a Bruker FRA 106 Raman module using the 1064 nm line of a Nd:YAG laser with 1 W. The samples were put in glass containers, which were placed in a tempered sample chamber equipped with a stirring unit.

Small angle scattering (SAXS) measurements were performed using a pinhole camera with a rotating anode generator and an area detector (Bruker AXS, Karlsruhe). All SAXS patterns were first corrected for background scattering from the experimental setup and then radially averaged to obtain the function $I(q)$, where $q = (4\pi/\lambda)\sin\theta$ is the scattering vector, 2θ being the angle between the incident and the diffracted beam and $\lambda = 0.154$ nm the X-ray wavelength. Spectra were obtained in the q-range from 0.15 to 9 nm^{-1} by combining data measured for two different sample−detector distances. The setup and its use for the investigation of porous materials are described in refs 4 and 5.

Following the method of Emmerling et al.,[6] the SAXS data were fitted using the following expression:

$$I(q) = I_0[B + V_0 S(q)P(q)]$$

where I_0 is a normalization constant depending on the setup, B a constant background from the sample, V_0 the mean volume of the primary particles, $P(q)$ their form factor, and $S(q)$ the structure factor describing the packing of the primary particles. Assuming nearly spherical primary particles with radius

(4) Fratzl, P.; Langmayr, F.; Paris, O. *J. Appl. Crystallogr.* **1993**, *26*, 820.
(5) Fratzl, P.; Vogl, G.; Klaumünzer, K. *J. Appl. Crystallogr.* **1991**, *24*, 588.
(6) Emmerling, A.; Petricevic, R.; Beck, A.; Wang, P.; Scheller, H.; Fricke, J. *J. Non-Cryst. Solids* **1995**, *185*, 240.

R, we can take:

$$V_0 = 4\pi R^3/3 \qquad P(q) = 1/[1 + \sqrt{2(qR)^2/3}]^2$$

$$S(q) = 1 + C(D)/(qR)^D$$

D being the fractal dimension of the aggregate and $C(D)$ a constant depending on D:[6] $C(D) = D\Gamma(D - 1)\sin[\pi(D - 1)/2]$. Hence, the fit yields three parameters, the background (B), the particle radius (R), and the fractal dimension (D). The fit was usually excellent over 4 orders of magnitude in the intensity and 2 orders of magnitude in q. Indeed, all the SAXS data follow Porod's law (that is, $I(q) \sim q^{-4}$ + constant) at large q (typically for $q > 0.5$ nm^{-1}). For all spectra, except AMMO10, the slope of the SAXS curve is smaller in the low-q region (see Figure 5), which enables the determination of R and D. In the case of AMMO10, the slope remains almost unchanged up to the smallest values of q. This means that the size of the particles is too large to be determined by SAXS in this case. It also turned out that the constant B was nearly the same for all samples (on the order of 0.02 nm^3). Since this parameter is not easily interpreted (and turns out to be a negligible contribution for $q < 3$ nm^{-1}), it will not be discussed further.

Results

When gels are prepared by base-catalyzed hydrolysis and condensation of $R_{nb}Si(OR)_3$/TMOS mixtures, gelation is retarded by an increasing portion of $R_{nb}Si(OR)_3$. In contrast, the gelation is strongly accelerated when TMOS is coreacted with $R_bSi(OMe)_3$, due to the basic properties of the functional groups. As a matter of fact, the reaction of AMMO/TMOS mixtures under the reaction conditions used for the $R_{nb}Si(OMe)_3$/TMOS mixtures resulted in the immediate formation of precipitates. The gel time can be increased by slightly acidic conditions or fluoride catalysis, and aerogels of the density ~0.1 g cm^{-3} were obtained by Hunt et al. from 9:1 mixtures of AMMO or AEAPS and TEOS under these conditions.[7] However, acid catalysis is detrimental to the formation of particulate gels.[8] Therefore, we exchanged TMOS by the slower reacting TEOS. Because of the low miscibility of TEOS, methanol, and water, we had to decrease the theoretical density of the aerogels to 0.1 g cm^{-3} (instead of 0.2 g cm^{-3}, mainly used for the $R_{nb}Si(OMe)_3$/TMOS mixtures), i.e., a larger portion of methanol was used. No catalyst was added, because the amino groups of the R_b substituent are an "internal catalyst".

With the basic properties of the groups R_b it seems surprising that, under these conditions, the gel times of $R_bSi(OMe)_3$/TEOS mixtures are *increased* when the portion of $R_bSi(OMe)_3$ is increased. For example, a 1:9 mixture of AMMO and TEOS gelled after 12 min, while it took 30 min for a 4:6 mixture. A solution of pure AMMO in aqueous methanol does not gel for days. On the other hand, a solution of pure TEOS in aqueous methanol is also stable in the absence of a catalyst.

The explanation for this behavior of AMMO- and AEAPS-containing mixtures is obtained by Karl Fischer titrations, exemplarily shown for AMMO/TEOS mixtures in Figure 1.

A solution of TEOS (without catalyst) did not consume water during the observation period. On the other hand,

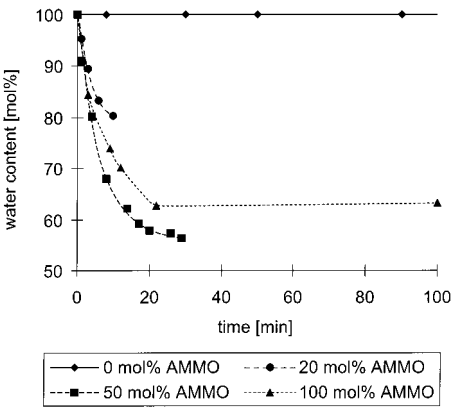

Figure 1. Karl Fischer titration of AMMO/TEOS mixtures for different portions of AMMO (0−100 mol %). The water content is given in percent of the initial amount.

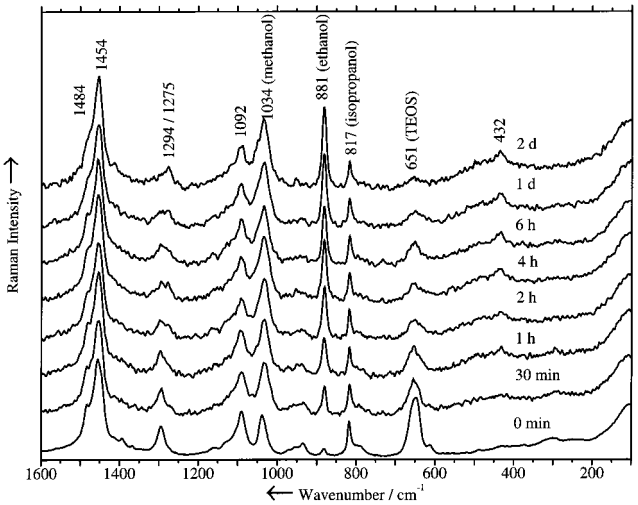

Figure 2. Change of the Raman bands in the range 200−1600 cm^{-1} for AEAPS10. The spectrum at $t = 0$ is that of the starting mixture before addition of water.

a solution of AMMO initially reacted rapidly with water. After some minutes the water concentration stayed constant, and the solution remained clear. No gel or precipitate was formed. It should be noted at this point that under the same experimental conditions (same solvent, silane:water ratio, and concentration) TEOS reacts only very slowly with water when a basic catalyst is added. When mixtures of AMMO and TEOS were employed, the initial water consumption was also rapid, but gels were formed, as described above. Thus, in the case of $R_bSi(OMe)_3$/TEOS mixtures, there is no direct correlation between the gel times and the kinetics of the water consumption.

Investigation of some $R_bSi(OMe)_3$/TEOS systems by Raman spectroscopy corroborated the fast reaction rates. Figure 2 exemplarily shows the change of the Raman bands for AEAPS10 within several hours after addition of water at $t = 0$. Due to the limited signal-to-noise ratio of the spectra, the overlapping $\nu_s(Si(OR)_4)$ band of TEOS (651 cm^{-1}) and the $\nu_s(Si(OR)_3)$ band of AEAPS (642 cm^{-1}) cannot be distinguished by a fitting procedure with a reasonably low error. However, hydrolysis can be qualitatively followed by the formation of ethanol [from TEOS; $\nu_s(CCO)_{sym}$) at 881 cm^{-1}] and the increase of the methanol $\nu_s(CO)$ band (from $R_bSi(OMe)_3$) at 1034 cm^{-1}. Both compounds are hydrolyzed

(7) Cao, W.; Hunt, A. J. *Mater. Res. Soc. Symp. Proc.* **1994**, *346*, 631.

(8) Wang, P.; Emmerling, A.; Tappert, W.; Spormann, O.; Fricke, J.; Haubold, H.-G. *J. Appl. Crystallogr.* **1991**, *24*, 777.

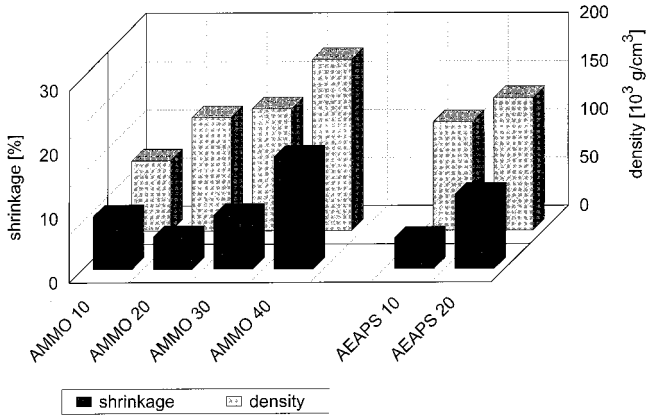

Figure 3. Shrinkage during supercritical drying and bulk density of the final aerogels depending on the portion of R_b-$Si(OR)_3$ in the starting mixture.

to a great extent already within the first hour. Despite the ethanol deformation band at 432 cm^{-1}, one can observe a broad band in the Si−O network region with a maximum around 435 cm^{-1}. This is an indication for the development of Q^4 units ($Si(OSi\equiv)_4$ units [9]) from the very beginning of the reaction.

Drying of the wet gels was performed with supercritical CO_2. Although we obtained mechanically stable aerogel bodies, the gels were more sensitive to small changes in the drying procedure than the gels derived from $R_{nb}Si(OMe)_3$, and fracture of the gel bodies during drying was more often observed. A possible reason could be reaction of CO_2 with the amino groups that could destabilize the gel network by breaking hydrogen bonds. In passing, it is worth mentioning that gels prepared by *acid*-catalyzed reaction of TEOS/AMMO mixtures were even less stable and gave only powders instead of monoliths upon supercritical drying.

Figure 3 shows the shrinkage during supercritical drying and the bulk density. Although the theoretical density was adjusted to 0.100 g cm^{-3}, the experimentally determined bulk densities of the final material were between 0.07 and 0.16 g cm^{-3}. The fact that the aerogel density of AMMO10 is below the theoretical density indicates that mass was lost during supercritical drying. Shrinkage was <10% for the AMMO10 and AEAPS10 samples and generally increased with an increasing $R_bSi(OMe)_3$ portion. Thus, the increasing density can be traced back to a decreasing volume of the aerogel bodies.

Chemical analysis allows a rough determination of the integrated portion of the functional silane (Figure 4). For calculating the theoretical values, complete integration of the functional organic groups and complete hydrolysis of all alkoxy groups was assumed. The observation that the values obtained from the carbon analyses are always higher than those from the nitrogen analyses shows that the real systems do not completely correspond to this ideal situation. However, the figures allow the conclusion that the integrated portion of amino groups is very high and the same for all samples except AMMO10. The high value of AMMO10 is probably due to the loss of unsubstituted oligomers from TEOS, which

(9) Lippert, J. L.; Melpolder, S. B.; Kelts, L. W. *J. Non-Cryst. Solids* **1988**, *104*, 139.

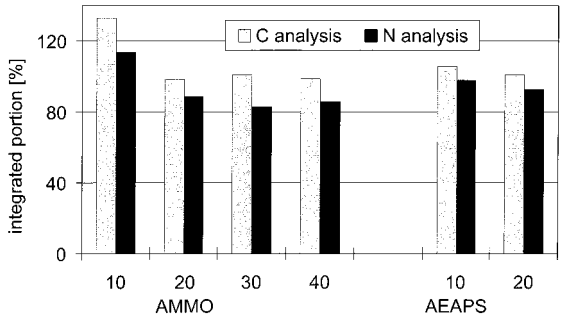

Figure 4. Portion of R_b groups integrated in the aerogels, determined by C and N elemental analysis. The numbers on the abscissa give the portion of $R_bSi(OR)_3$ in the starting mixture.

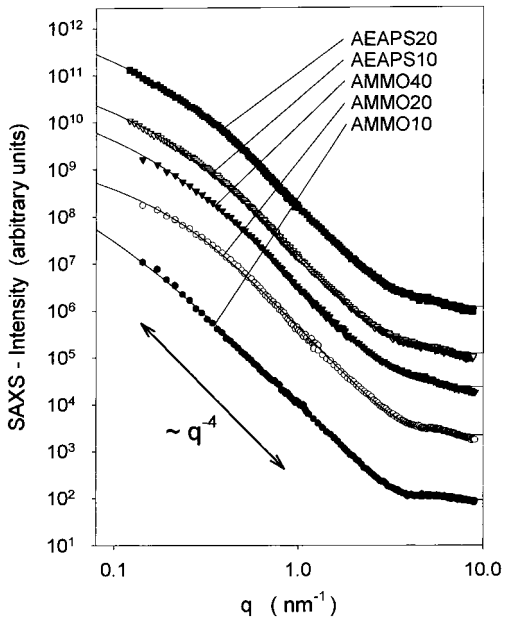

Figure 5. SAXS intensity, $I(q)$, as a function of the scattering vector, q, for selected aerogels. The data are plotted on double-logarithmic scales and are shifted vertically for clarity. The full lines show the fits used to determine particle radius R and fractal dimension D for each sample. Porod's law (that is, a slope of −4 in this graph) is indicated by the double arrow. Note that AMMO10 follows Porod's law almost up to the smallest q values. Hence, no reliable data for the particle radius could be obtained in this case, except that it must be much greater than for the other aerogels.

increases the relative carbon content in the aerogels. This correlates with the low density of this sample.

The structure of the resulting aerogels was investigated by nitrogen sorption, small-angle X-ray scattering (SAXS), and transmission−electron microscopy (TEM). The results are presented in Table 2 and Figures 5 and 6. The hysteresis of the adsorption/desorption isotherms had the same shape as that of unmodified silica aerogels, but no maximum could be observed in the pore radii distribution (determined according to the BJH method) between 1 and 50 nm. The specific surface areas of the samples were significantly lower than for an unmodified silica aerogel or the aerogels obtained from $R_{nb}Si(OR)_3$/TMOS mixtures and do not correlate with the portion of $R_bSi(OMe)_3$ employed in the alkoxysilane mixture. We have previously shown for the aerogels prepared from $R_{nb}Si(OR)_3$/TMOS mixtures that the values obtained for the pore volume from nitrogen

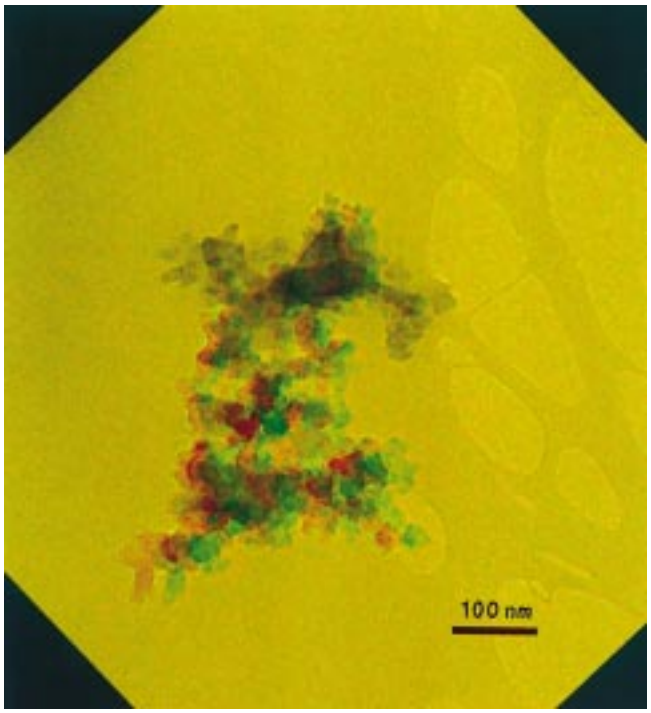

Figure 6. Transmission electron micrograph of AMMO10. To get a three-dimensional image, the figure must be viewed through a a pair of red (left eye)−green (right eye) glasses.

sorption experiments are unrealistic, because the aerogel network is deformed during the measurements.[3] As shown by Scherer et al. this results in an underestimation of the specific pore volume.[10] Severe compression of the gel network was also observed for the aerogels prepared in this work.

The radius (R) of the primary particles as well as the fractal dimension (D) of their aggregates was determined by SAXS. The scattering curves are shown in Figure 5, and the derived parameters are listed in Table 2.

Particles with radii of 6.0−6.3 nm were obtained for AMMO20, AMMO40, AEAPS10, and AEAPS20. The fractal dimension D of these samples, which is a measure for the degree of branching of the network formed by the primary particles, had values in the range 1.26−1.55. The scattering curve of AMMO10 has a different appearance (slope proportional to q^{-4}) which does not provide information about the particle radii and the fractal dimension. However, the SAXS curve shows that the particles of AMMO10 are larger than those of the other samples.

The transmission−electron micrograph of AMMO10 (Figure 6) corroborates that the network of this aerogel is formed from rather large particles of about 25 nm in diameter. Figure 7 shows an aerogel with a density of 0.248 g cm^{-3} prepared from a 9:1 mixture of TMOS and $(MeO)_3Si(CH_2)_3SH$, for comparison (particle diameter from TEM, 7−8 nm; particle diameter determined from SAXS, 6.8 nm). The micrographs were taken at an acceleration voltage of 120 kV; both samples were stable in the electron beam, i.e., the aggregates did not change their shape and size. The structural difference between both samples is obvious, although both show the typical aerogel network of loosely connected primary particles.

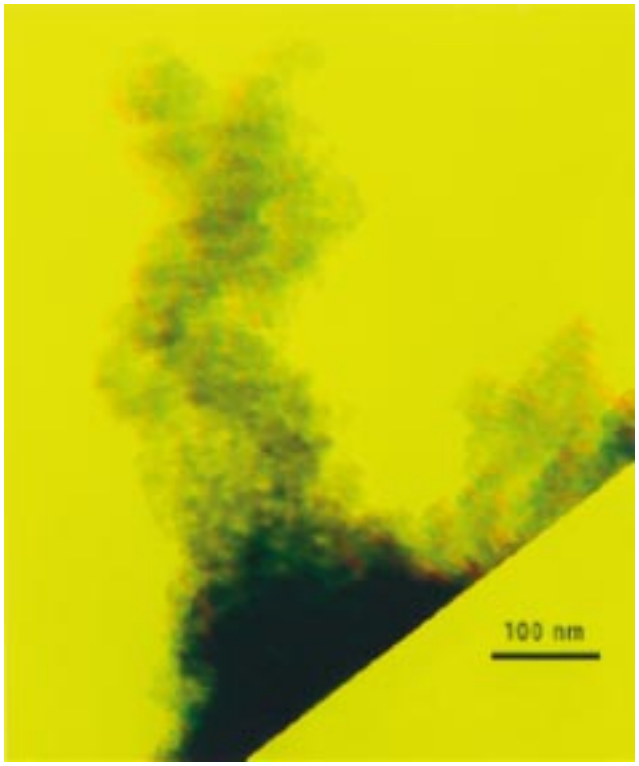

Figure 7. Transmission electron micrograph of an aerogel prepared from $Si(OMe)_4/(MeO)_3Si(CH_2)_3SH$ (9:1). To get a three-dimensional image, the figure must be viewed through a a pair of red (left eye)−green (right eye) glasses.

Because the TEM micrographs represent projections of the structure onto the image plane, the network branching in space, i.e., the spatial arrangements of the primary particles, is difficult to image. Therefore, electron micrographs were recorded as stereopairs with a difference in the illumination or projection angle of 3−6°. Colored images are composed from two stereo images, one printed in red and the other in green.

Discussion

The gelation behavior of TEOS/AMMO or TEOS/AEAPS mixtures corresponds neither to that of $Si(OR)_4/R_{nb}Si(OR)_3$ mixtures nor to that of TEOS under strongly basic conditions.[11] Addition of water to AMMO or AEAPS [in the absence of $Si(OR)_4$)], on the other hand, gave clear solutions and no gels, while a 1:1 mixture of $PrSi(OMe)_3$ and amines (simulating both parts of bifunctional $R_bSi(OMe)_3$ in two different molecules) resulted in the immediate formation of precipitates. It is known from the literature that AMMO quickly reacts with water, but no gel is formed. The hydrolysis behavior of AMMO solutions [in the absence of $Si(OR)_4$] was explained by the formation of intramolecular hydrogen bonds in the hydrolyzed species (Chart 1) which inhibit formation of the gel network.[12]

(10) Scherer, G. W.; Smith, D. M.; Stein, D. *J. Non-Cryst. Solids* **1995**, *186*, 309.

(11) Matsoukas, T.; Gulari, E. *J. Colloid Interface Sci.* **1988**, *124*, 252.

(12) Plueddemann, E. P. *Silane Coupling Agents*; Plenum Press: New York, 1991. Rousseau, C.; Poinsignon, C.; Garcia, J.; Popall, M. *Chem. Mater.* **1995**, *7*, 828. van Blaaderen, A.; Vrij, A. *J. Colloid Interface Sci.* **1993**, *156*, 1. Hoebbel, D.; Pitsch, I.; Jancke, H.; Costisella, B. *Z. Anorg. Allg. Chem.* **1990**, *588*, 199. Zhmud, B. V.; Sonnefeld, J. *J. Non-Cryst. Solids* **1996**, *195*, 16.

Chart 1

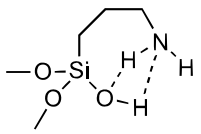

In the presence of TEOS, i.e., when TEOS/$R_bSi(OMe)_3$ mixtures are reacted, gels were formed within a few minutes, although only a small amount of water was consumed (Figure 1). One of the reasons for the rapid formation of gels may be the catalysis of TEOS hydrolysis and condensation by the amino groups of $R_bSi(OMe)_3$. Furthermore, the *inter*molecular formation of hydrogen bridges between the amino groups of AMMO or AEAPS and silanol groups of $Si(OEt)_{4-x}(OH)_x$ could promote gel formation. Although *intra*molecular hydrogen bonds (Chart 1) are entropically favorable, the OH groups attached to Q silicon atoms are more acidic than those attached to T silicon atoms and therefore should preferentially act as hydrogen donors in hydrogen bonds. Hydrogen bonding could also explain why TEOS is completely incorporated in the gels when the concentration of $R_bSi(OMe)_3$ is high. In the AMMO10 sample there may not be enough amino groups to hydrogen bond all dissolved monomeric or small oligomeric species derived from TEOS. These may become entrapped in the pores of the rapidly formed gel network and washed out during supercritical drying.

With these notions one would expect that an increasing portion of $R_bSi(OR)_3$ would shorten gelation times. The contrary is observed, probably because of the decreasing portion of network-forming units and the redissolution of siloxane units. Thus, an increasing $R_bSi(OR)_3$ portion in the $Si(OR)_4/R_bSi(OR)_3$ mixtures has two contrasting effects on the gelation behavior: a higher amino group concentration acting as catalysts and hydrogen-bond acceptors vs a lower portion of network-forming units. The latter is also reflected in the larger shrinkage of the gel bodies during aging and supercritical drying when the $R_bSi(OMe)_3$ portion is increased (Figure 3). Shrinkage is qualitatively related to the stability of the gel network.

In the aerogels prepared from TMOS/$R_{nb}Si(OR)_3$, the functional organic groups were only completely incorporated when the $R_{nb}Si(OR)_3$ portion was $\leq$10%. The portion of the incorporated groups decreased with an increasing portion of $R_{nb}Si(OR)_3$ in the starting mixture. This observation was explained by the two-stage growth model, where some saturation behavior is expected. A possible explanation for the complete incorporation of AMMO and AEAPS into the gels even if their portion in the starting mixture is as high as 40% is that the reaction rates of $R_bSi(OMe)_3$ with water are very high and in the same magnitude as that of TEOS under these conditions. Therefore, the two-stage model cannot be applied any longer.

The Raman spectroscopic investigations indicate that highly branched units (Q^4) are probably formed in a very early stage of the overall reaction, as expected for the reaction of tetraalkoxysilanes with water under strongly alkaline conditions. Such conditions are known to lead to particulate gels with large primary particles and large pores.[8,13] Large particles are indeed found by SAXS and TEM (Table 2 and Figure 6). However, contrary to the aerogels prepared from $R_{nb}Si(OR)_3$/TMOS mixtures, the particle radii (R) in the aerogels prepared from AMMO or AEAPS apparently do not depend on the $R_bSi(OMe)_3$ portion in the starting mixture, which supports the previously discussed notion that both silanes are involved in the formation of the gel network. The specific surface areas σ (Table 2), which are rather low for aerogels of that density, are consistent with the relatively large particle radii. For comparison, the specific surface areas of aerogels with the same density, prepared from $R_{nb}Si(OR)_3$/TMOS mixtures, were in the range of 350−690 $m^2\ g^{-1}$ [depending on the $R_{nb}Si(OR)_3$ portion].

AMMO10 is an exception. A possible explanation for the larger particles is that this system basically behaves like a TEOS solution in the presence of a high concentration of a base catalyst, which is known to lead to large particles. In systems with higher portions of AMMO, or in the AEAPS systems with the larger organic groups, a high steric barrier against particle aggregation is created, and small particles are thus stabilized.

The value $3/R$ (i.e., the surface-to-volume ratio for a sphere) can be understood as the internal surface area per skeletal unit volume of the aerogel. The average value of $3/(R\sigma)$, which can be interpreted as the skeletal density, is 1.58 g cm^{-3}. The skeleton density of unmodified silica aerogels is in the range of 2.0−2.2 g cm^{-3}; in organically modified silica somewhat lower values can be expected. In the aerogels prepared from $R_{nb}Si(OR)_3$/TMOS mixtures, an average skeleton density of 1.43 g cm^{-3} was observed.[3]

The C parameter reflects the polarity of the surface. Typical values are 120 for unmodified silica aerogel (polar surface) and 30 for unpolar surfaces of modified silicas.[14] The C values for the aerogels prepared from AMMO and AEAPS surprisingly indicate that the surface is rather unpolar. One would intuitively expect higher values due to the polar amino groups, which should strongly interact with the nitrogen molecules used for the sorption experiments. A possible explanation is that the amino groups hydrogen bond to surface silanol groups or among each other and the N_2 molecule therefore only gets in contact with the unpolar propylene spacer. No saturation behavior of the C parameter was observed as for the aerogels prepared from $R_{nb}Si(OR)_3$/TMOS mixtures, when the portion of the trialkoxysilane was increased. This is additional evidence that the network-forming process in $R_bSi(OMe)_3$/TEOS mixtures is different and does not proceed in a stepwise manner.

The fractal dimensions (1.26−1.53) indicate that the network is formed by cluster−cluster aggregation rather than monomer−cluster aggregation. A smaller mass fractal dimension than about 2.3 is explained by the kinetic growth models by the predominance of cluster−cluster condensation.[13] This happens if hydrolysis is fast compared to condensation.

The low fractal dimensions show that the role of AMMO and AEAPS in the $R_bSi(OMe)_3$/TEOS mixtures

(13) Schaefer, D. W. *Science* **1989**, *243*, 1023. *MRS Bull.* **1994**, *24* (4), 49. Keefer, K. D.; Schaefer, D. W. *Phys. Rev. Lett.* **1986**, *56*, 2199, 2376.

(14) Lowen, K. W.; Broge, E. C. *J. Phys. Chem.* **1961**, *65*, 16.

is not just that of a catalyst for the hydrolysis and condensation of TEOS. In this case larger particles with a higher fractal dimension would be expected. For example, an aerogel with a bulk density of 0.341 g cm^{-3} prepared from only TMOS in the presence of a *catalytic* amount of ammonia under identical conditions and supercritically dried with CO_2 had a fractal dimension of 2.76.[15] The low fractal dimensions of the aerogels prepared in this work are another indication that both TEOS and $R_bSi(OMe)_3$ are involved in the initial network formation process.

Conclusions

Base-catalyzed sol−gel processing of $R'Si(OR)_3/Si(OR)_4$ mixtures, in which the organic group has no strongly basic substituent, results in gel networks with a structure that can be explained by a two-stage process. In the first stage, the network is formed from the tetraalkoxysilane, to which then the $R'SiO_{3/2}$ units condense.[2,3] The network-forming process is clearly different when the organic group R′ contains a basic substituent, as in AMMO or AEAPS. All structural parameters are consistent with the notion that $R_bSi(OR)_3$ and $Si(OR)_4$ are involved in the build-up of the gel network. Hydrogen bonds between the amino groups and the OH groups of (partially) hydrolyzed species from $Si(OR)_4$ possibly play a major role.

Acknowledgment. The work of N.H. and U.S. was financially supported by the Fonds zur Förderung der wissenschaftlichen Forschung (FWF) and the Hoechst AG, and that of B.R. and W.K. by the Deutsche Forschungsgemeinschaft. N.H. and U.S. thank Prof. Jochen Fricke (Physics Institute, University of Würzburg) and co-workers for the cooperation and fruitful discussions. SAXS measurements were started at the Materials Physics Institute of the University of Vienna (R.M. and P.F.). R.M. was supported by a grant from the "Aktion Österreich-Ungarn".

CM980756L

(15) Schwertfeger, F. Diplomarbeit, Universität Würzburg, 1991.